Available online at www.sciencedirect.com
SCIENCE DIRECT®
Advances in Space Research 36 (2005) 1050–1056
ADVANCES IN SPACE RESEARCH (a COSPAR publication)
www.elsevier.com/locate/asr

The galactic first-look survey with the *Spitzer* space telescope

Martin J. Burgdorf [a,c,*,1], Martin Cohen [b], James G. Ingalls [c], S. Ramirez [d], Jeonghee Rho [c], S.R. Stolovy [c], Sean J. Carey [c], S.B. Fajardo-Acosta [c], W.J. Glaccum [c], G. Helou [c], D.W. Hoard [c], J. Karr [c], P.J. Lowrance [c], J. O'Linger [c], Deborah L. Padgett [c], W.T. Reach [c], L.M. Rebull [c], John R. Stauffer [c], S. Wachter [c]

[a] *Astrophysics Research Institute, Liverpool John Moores University, Twelve Quays House, Egerton Wharf, Birkenhead CH41 1LD, UK*
[b] *Monterey Institute for Research in Astronomy, 200 Eighth Street, Marina, CA 93933, USA*
[c] *Spitzer Science Center, California Institute of Technology, Division of Physics, Mathematics and Astronomy, 1200 California Blvd, 220-6, Pasadena, CA 91125, USA*
[d] *Infrared Processing and Analysis Center, California Institute of Technology, 100-22, Pasadena, CA 91125, USA*

Received 1 October 2004; received in revised form 11 May 2005; accepted 18 May 2005

Abstract

The galactic first look survey (GFLS) of the *Spitzer* space telescope was executed during 1–11 December 2003 as one of the first science observations during nominal operations. The aim of the FLS is to provide a characteristic "first-look" at the mid-and far-infrared sky at sensitivities that allow the detection of point sources ≈100 times fainter than those in previous systematic large-area surveys. The whole program took 35.5 h to complete and consisted of the following elements:

- Galactic longitudinal strips of size $15' \times 1°$ with IRAC and MIPS at $l = 105.6°$ and 254.4° and various galactic latitudes.
- $10' \times 10'$ IRAC maps at $l = 97.5°$ and $b = 0°$, ±4°, and +16°.
- Coverage of L1228 with 2° scan maps.

Even at these large distances from the galactic center, confusion sets a limit to the detection of point sources in the galactic plane for IRAC channel 1 (3.6 μm) at 100 μJy ≈ 16.1^m. As positive galactic latitudes were mainly sampled at $l = 97.5°$ and 105.6° and negative latitudes at 254.4° galactic longitude, the observations are well suited to derive information on the warp of the galactic disk. In order to reproduce the source counts from the GFLS we had to assume an amplitude of the warp within 20% of that derived from 2MASS.

The whole survey is included in the *Spitzer* science archive which opened in April 2004.

Keywords: Milky Way; IR; *Spitzer*; Surveys

1. Introduction

In order to quickly provide the *Spitzer* user community with representative data from this observatory, the *Spitzer* science center (SSC) conducted a first-look survey among the first science tasks during nominal operations, which started on day 98 of the mission. The survey consisted of an ecliptic, a galactic, and an

* Corresponding author. Tel.: +44-151-231-2903; fax: +44-151-231-2921.
E-mail address: burgdorf@ipac.caltech.edu (M.J. Burgdorf).
[1] The research described here was based on observations obtained with the *Spitzer* Space Telescope, which is operated by the Jet Propulsion Laboratory, California Institute of Technology, under NASA contract 1407.

0273-1177/$30
doi:10.1016/j.asr.2005.05.064

extragalactic component. The FLS is the inaugural Director's Discretionary Time program.

The primary goals of this ≈110-h survey were (1) to provide a characteristic "first-look" at the mid-infrared sky at sensitivities that allow the detection of point sources about 100 times fainter than those in previous systematic large-area surveys; and (2) to rapidly process the data and place it into the public domain in time to impact early *Spitzer* investigations.

With the galactic FLS we tried to serve the *Spitzer* user community by characterizing the cirrus and background source counts at low galactic latitudes and toward a molecular cloud. This information is essential for calculating the confusion noise in observations close to the galactic plane and for estimating fluctuations in regions with diffuse emission. In order to put the selected regions probed with the galactic FLS into context, we compared the results from our observations with a model of the point source sky.

Compared to surveys of the galaxy at similar wavelengths with the infrared space observatory, e.g., GPSURVEY (Burgdorf et al., 2000) or ISOGAL (Schuller et al., 2003), the galactic FLS with *Spitzer* was 100–250 times more sensitive: $\leqslant 100$ μJy with the Infrared Array Camera (IRAC) between 3.6 and 8 μm. Many objects were found in the images from the galactic FLS which by themselves constituted interesting discoveries. Some examples of these findings are described in the following.

2. Observations

A third of the time for the whole FLS was allotted to its galactic component. Different galactic environments were probed with the following observations:

- Multiband imaging photometer for *Spitzer* (MIPS) and infrared array camera maps (each roughly $15' \times 1°$) at $l = 254.4°$, $b = 0°$, $-2°$, $-5°$, $-9°$, $-14°$ and $l = 105.6°$, $b = -1.3°$, $0.3°$, $2°$, $4°$, $8°$, $16°$, $32°$ in order to check the symmetry of our galaxy that is assumed in its model.
- Small IRAC maps at $l = 97.5°$, $b = 0°$, $\pm 4°$, $16°$ in order to characterize background source counts purely in the disk.
- MIPS and IRAC maps (roughly $10' \times 2°$) across the center of Lynds 1228 and lower emission regions in order to characterize a molecular cloud (see Fig. 1).

The selection of the coordinates for this survey was guided by the aims mentioned in the previous section, which required an unbiased survey of the galactic disk. One had to steer clear of very bright objects in order to avoid saturation of the detectors, and no duplication of observations in the *Spitzer* reserved observations catalog was allowed. Besides, the pointing constraints of *Spitzer* had to be taken into account. These requirements excluded in particular the inner galactic disk from the galactic FLS, which was mapped by the Galactic Legacy Infrared Mid-Plane Survey Extraordinaire (Benjamin et al., 2003).

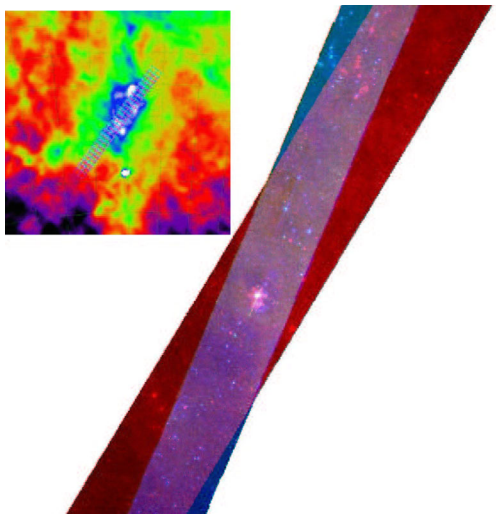

Fig. 1. False three-color image of the central region of the L1228 cloud, where blue = IRAC2 (4.5 μm), green = IRAC4 (8 μm) and red = MIPS (24 μm). Inset: a visualization of these observations on an IRAS 100μm image: cyan = 3.6/5.8 μm magenta = 4.5/8 μm. The raster map is centered on R.A. $20^h57^m12^s$ and Dec. $+77°35'48''$ (J2000) and its size is roughly $10' \times 120'$. North is on top. (For interpretation of the references to colour in this figure legend, the reader is referred to the web version of this article.)

Most of the point sources detected in all directions in the IRAC filters lie in the galactic disk. The contribution from the arms is comparatively small, in particular for the galactic longitude $l = 97.5°$ (Drimmel and Spergel, 2001, 1992). The fields at $l = 97.5°$, $b = 0°$ and $l = 105.6°$, $b = 0.3°$ have some overlap with the ISOGAL survey; they were used to check the absolute accuracy of the photometric calibration of the FLS data (15%) against earlier observations. The direction $l = 254.4°$ lies in the "Orion spur", thus introducing an element of galactic structure to the survey that is missing in the other directions.

The different galactic latitudes probed with the galactic FLS arc needed to determine how the density of point sources depends on the distance from the plane. The line of sight within the disk was roughly cut in half from one latitude to the next. Galaxies dominate the source counts at 24 μm in the fields at the highest galactic latitudes. Two pairs of directions in the galactic FLS, $(97.5°, -4°)/(97.5°, 4°)$ and $(254.4°, -2°)/(105.6°, 2°)$, are suited to check how symmetric the galactic disk is with respect to the plane and the galactic center.

Mosaics were made of the pipeline basic calibrated data (BCD) images using the SSC's MOPEX package (publicly available at `ssc.spitzer.caltech.edu`). We first performed a cosmetic fix of the multiplexer

bleed and the column pulldown produced in the IRAC data by bright sources to improve the data products. An overlap correction was applied to match the background in the overlapping regions of single BCDs. A mosaic was created for each band, correcting for cosmic rays and other artifacts using radhit and dual outlier rejection capabilities of MOPEX. The source extraction was done on the individual BCDs using APEX (the point source extractor included in the MOPEX package). The source extraction process rejects the cosmic rays and the other artifacts identified in the creation of the mosaics. The flux of the sources comes from a point response function (PRF) fitting process for most of the sources. For the sources where the PRF fitting process was not successful, we derived fluxes using aperture photometry by first subtracting out a smoothed background and then integrating the flux within a fixed aperture. For a general discussion of the calibration and data reduction of IRAC and MIPS see Fazio et al. (2004) and Rieke et al. (2004).

The MIPS 24 μm strips at $l = 254.4°$ and $l = 105.6°$ were analyzed to characterize the diffuse interstellar emission. The strips crossed a number of known molecular and atomic clouds, including 13 Lynds Dark Nebulae (Lynds, 1962), the Cepheus Flare, and the Gum Nebula. The power spectral analysis of the GFLS region centered on G254.4-9.0, part of the Gum Nebula, was described in Ingalls et al. (2004). Here we summarize the spatial statistics of 24 μm emission for all 10 diffuse fields in the strips with detectable signal. The area analyzed encompasses a total of 2.66 square degrees, or about 0.01% of the sky. Reduction of the survey data for characterization of diffuse emission was done as described by Ingalls et al. (2004). The emission from point sources was characterized and removed using the StarFinder code written in IDL (Diolaiti et al., 2000a,b). The images were then filtered to remove instrumental noise using a multiresolution wavelet technique (Starck and Murtagh, 1998). Radial power spectra for each of the images were computed by squaring the amplitudes of the image Fourier transforms, and azimuthally averaging in equally spaced wavenumber bins. The spectra were normalized using Parseval's relation in two dimensions, i.e., the average power in Fourier space equals the total variance in the original image.

3. Results

3.1. Source counts

Fig. 2 shows a comparison between the point source density in the galactic plane found with *Spitzer* and the values calculated with the SKY model for $l = 105.6°$, $b = 0.3°$. SKY is a physically realistic model for the point source sky capable of predicting source counts from the far-UV to the mid-IR. SKY has been tested extensively against counts from IRAS, MSX, ISO, and 2MASS, and operates in all the IRAC and MIPS 24 μm bands with an absolute calibration basis identical to that of the *Spitzer* instruments (Wainscoat et al., 1992; Cohen, 1993, 1994, 1995). IRAC1 (3.6 μm) is the band that is most sensitive to stars, but the agreement between model and observations is similar at the other wavelengths. There is also good agreement between the source fluxes obtained with ISOGAL and the brightest objects detected with IRAC3/4.

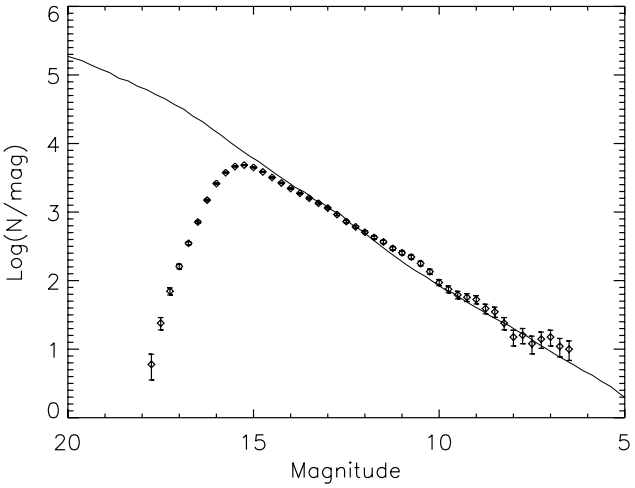

Fig. 2. Comparison of SKY modeled and galactic FLS observed differential star counts at $l = 105.6°$, $b = 0.3°$ with IRAC channel 1. Poisson error bars are shown, appropriate to the actual number of sources observed in each bin. Diamonds, observed star counts; solid line, model prediction.

Observations at the same longitude, but higher galactic latitudes, produce larger numbers of point sources than would be expected on the basis of a flat disk (see Fig. 3). This is due to the warp which moves the mean position of the disk to positive heights at longitudes 97.5° and 105.6° and to negative heights at $l = 254.4°$. A better agreement between observations and model is achieved with a modification of the average elevation of the disk in SKY according to formula 20 in López-Corredoira et al. (2002). The amplitude of the warp has to be within 20% of that derived by López-Corredoira et al. (2002) from 2MASS data in order to be compatible with the IRAC1 source counts.

At 24 μm, the agreement between SKY and observations is only good near the galactic plane. The larger the value of $|b|$, the greater becomes the contribution of galaxies to the "point" source counts, resulting in an excess of actually observed objects compared to the model of our galaxy (see Fig. 4). For a discussion of galaxy counts as a function of mid-infrared fluxes see Marleau et al. (2004). We assumed the conversions between Jy and mag shown in Table 1.

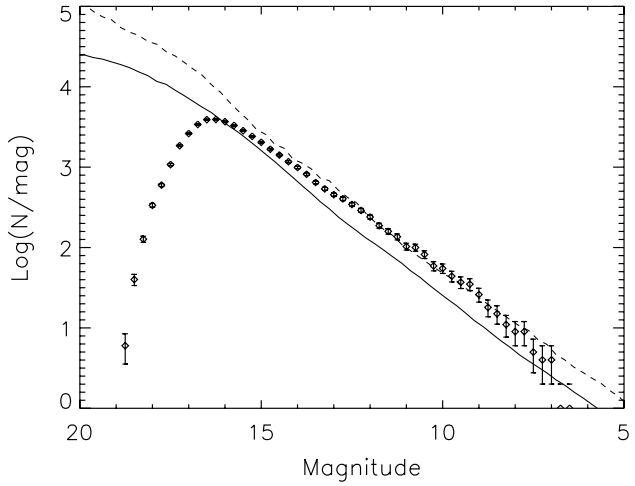

Fig. 3. Comparison of SKY modeled and galactic FLS observed differential star counts at $l = 105.6°$, $b = 8°$ with IRAC channel 1. Poisson error bars are shown, appropriate to the actual number of sources observed in each bin. Diamonds, observed star counts; solid line, model prediction for flat disk; dashed line, model prediction for warped disk.

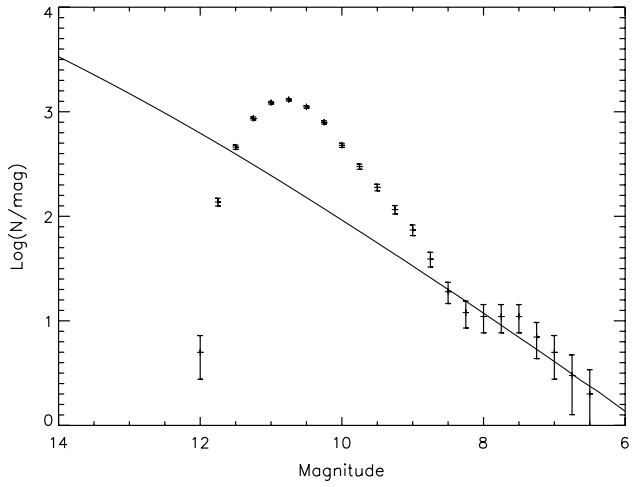

Fig. 4. Comparison of SKY modeled and galactic FLS observed differential star counts at $l = 105.6°$, $b = 32°$ with MIPS24. Poisson error bars are shown, appropriate to the actual number of sources observed in each bin. Plus signs, observed star counts; solid line, model prediction for galactic sources only.

Table 1
Zero magnitude fluxes

Channel	Wavelength (μm)	Flux (Jy)
IRAC1	3.6	277.5
IRAC2	4.5	179.5
IRAC3	5.8	116.6
IRAC4	8.0	63.1
MIPS24	24	7.3

3.2. Individual fields

3.2.1. Lynds 1188

Fig. 5 shows a three-color image of the field $l = 105.6°$, $b = 4°$. It lies at the edge of the "Cepheus bubble", a huge dust ring around an OB association (Ábráham et al., 2000). Two new groups of young stellar objects (YSOs) were found in this area and identified as such from their 1–24 μm spectral energy distributions. The distances derived from CO velocity data from the Canadian galactic plane survey are 900 and 6700 pc for the group at higher and lower latitude, respectively. 900 pc is the distance to the Cepheus Bubble (Kun et al., 1987). The other group of YSOs might lie in the outer arm (Rebull et al., 2004).

3.2.2. $l = 254.4°$, $b = 0°$

The field $l = 254.4°$, $b = 0°$, shown in Fig. 6, is a particularly good example of the potential for new discoveries in the galactic FLS. It contains an HII region which was until now not identified as such and a possible supernova remnant. The HII region has a diameter of a few arcmin; its central star is CD-354469. The other new source is also diffuse and bright in the mid-infrared, with a radio spectral index of 0 ± 0.2. This indicates that it is either a Crab-like supernova remnant or an HII region (Rho et al., 2004).

3.2.3. Lynds 1228

A small group of young stellar objects was discovered in the map of L1228 that was taken in the galactic FLS. The fluxes of IRAS sources in this area are too high due to confusion, but with the data from *Spitzer* it was possible to determine reliable spectral energy distributions, and a diversity of evolutionary states of the disks was found for the stars in this aggregate (Padgett et al., 2004).

3.3. Cirrus structure and confusion noise

Table 2 lists the region centers, the sizes of the areas analyzed, the radial power spectral indices, β, and the estimated confusion noise in the fields, σ_{cn}. The spectral indices were derived from power law fits of the form $P(k) = P_0(k/k_0)^{-\beta}$, where P_0 is the power spectrum value at the fiducial wavenumber, k_0. For this work we use $k_0 = 0.1$ arcsec^{-1}. Error bars in β are formal fit uncertainties. In 7 out of 10 fields, the spectra showed an obvious break into two power laws, with the difference in indices being close to unity in 5 cases. This implies a transition from a 2D to 3D structure in the emitting regions. See Ingalls et al. (2004) and references therein for more on the implications of a spectral break. When two spectral indices were measured, we listed both of the indices in Table 2, with the low k indices printed above the high k indices.

The noise due to spatially correlated cirrus emission or confusion noise, was computed in the observed fields using a formula based on that derived in Gautier et al. (1992):

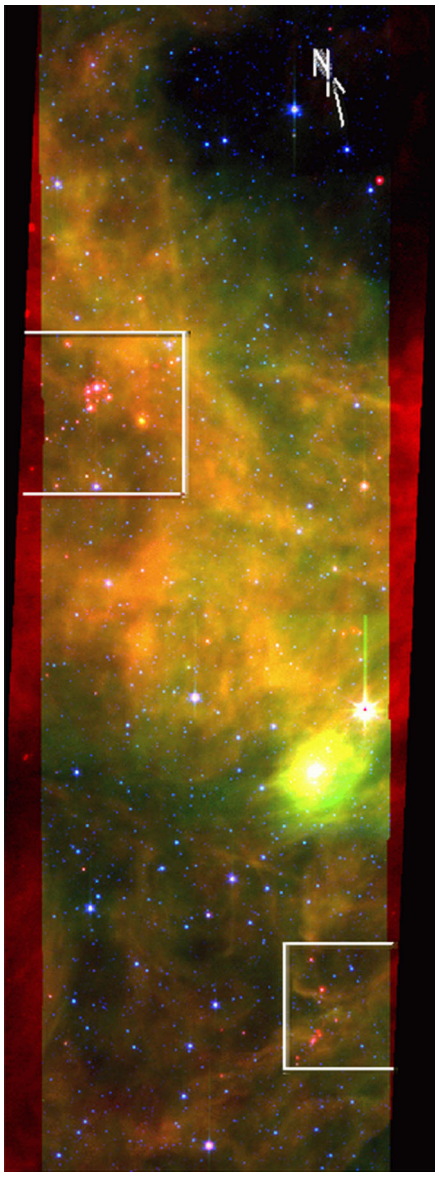

Fig. 5. Three-color plot of the field $l = 105.6°$, $b = 4°$ with IRAC and MIPS: blue = 3.6 μm, green = 8 μm, red = 24 μm. The image is centered on R.A. $22^h17^m00^s$ and Dec. +61°33′36″ (J2000) and its size is roughly $15' \times 60'$. The two white rectangles indicate the positions of the newly discovered clusters of young stars in this image, appearing red. (For interpretation of the references to colour in this figure legend, the reader is referred to the web version of this article.)

$$\left(\frac{\sigma_{\rm cn}}{\mu{\rm Jy}}\right) = 6.65 \times 10^{-8} 10^{E_0} \left(\frac{d}{60\ {\rm arcsec}}\right)^{3-\beta/2} \times \left(\frac{60 k_0}{{\rm arcmin}^{-1}}\right)^{-\beta} \left[\frac{P_0}{({\rm MJy\ sr}^{-1})}\right]^{1/2}.$$

Here, E_0 is a function that depends on the spectral index, the ratio of aperture size to telescope resolution, and the ratio of aperture size to separation distance between source and background measurements. Values of E_0 for various observing configurations, normalized to $k_0 = 1\ {\rm arcmin}^{-1}$, were tabulated as a function of β in

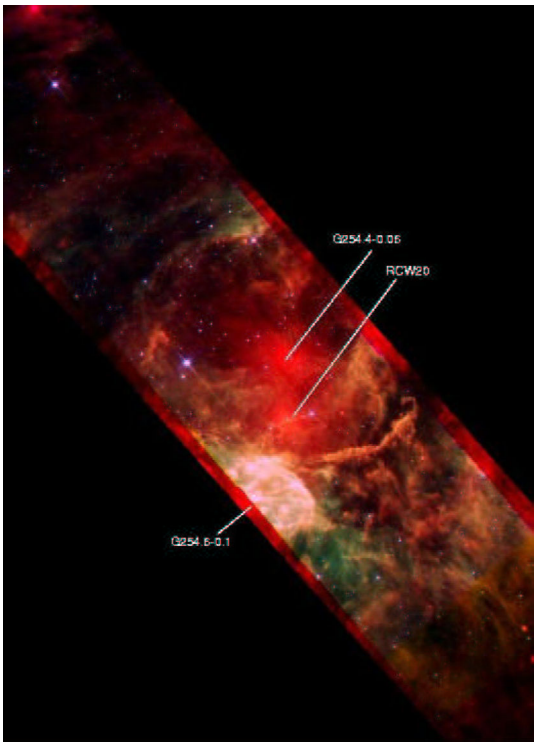

Fig. 6. Three-color plot of the field $l = 254.4°$, $b = 0°$ with IRAC and MIPS: blue = 4.5 μm, green = 8 μm, red = 24 μm. The image is centered on R.A. $18^h02^m26^s$ and Dec. −23°00′39″ (J2000) and its size is $35' \times 35'$. There are two HII regions in this image: RCW20 and G254.4-0.06, the latter of which is newly identified; G254.6-0.1 is either a supernova remnant or another HII region. North is on top. (For interpretation of the references to colour in this figure legend, the reader is referred to the web version of this article.)

Table 2
24 μm spatial statistics of GFLS fields

Field center	Approx. size (deg)	β	$\sigma_{\rm cn}$ (μJy)
G105.6 − 1.3	1.02 × 0.22	−2.31 ± 0.09	8.89
		−3.38 ± 0.02	4.67
G105.6 + 0.35	0.68 × 0.25	−3.12 ± 0.03	4.42
G105.6 + 2.0	1.51 × 0.18	−3.00 ± 0.04	6.86
G105.6 + 4.0	0.68 × 0.20	−3.24 ± 0.08	6.81
		−4.15 ± 0.04	5.39
G105.6 + 8.0	1.04 × 0.12	−2.19 ± 0.04	2.47
		−2.8 ± 0.3	2.57
G105.6 + 16.0	1.51 × 0.25	−2.23 ± 0.03	3.08
		−3.18 ± 0.05	4.09
G254.4 − 9.0	0.54 × 0.25	−2.76 ± 0.12	6.73
		−3.67 ± 0.03	4.04
G254.4 − 5.0	1.51 × 0.25	−2.45 ± 0.02	3.32
G254.4 − 2.0	0.82 × 0.20	−2.31 ± 0.02	2.38
		−3.13 ± 0.10	2.69
G254.4 + 0.0	1.51 × 0.20	−2.66 ± 0.07	37.6
		−3.67 ± 0.04	24.7

Gautier et al. (1992). Here we allow for different values of k_0. In estimating E_0 we assumed that the source emission was measured in an aperture with diameter d, equal to the size of the MIPS 24 μm beam profile, and the background is measured in an annulus of radius $4d$ and thickness d. Since we normalized our power spectra to the variance in image surface brightness, this formula includes a scaling by the source aperture solid angle $\pi d^2/4$. For the fields in which we measured a break in the power spectrum, we calculated separate σ_{cn} estimates from the separate power law fits.

Since our data have much higher spatial resolution than early cirrus surveys with *IRAS*, we can test predictions of the confusion noise made by extending the *IRAS* power spectrum to the small-scale regime. The 24 μm cirrus confusion noise in the fields analyzed ranges from about 2 to 40 μJy, much higher than the value $\sigma_{cn} = 0.06$ μJy predicted for a typical cosmological field (Dole et al., 2003). This is not surprising, since the GFLS regions analyzed have strong galactic emission. To assess the confusion noise in a standard extragalactic field, we have performed power spectral analysis of the cirrus emission in the *Spitzer* 24 μm image observed as part of the extragalactic first look survey, a $2° \times 2°$ region centered at R.A. $17^h18^m00^s$ and Dec. $+59°30'00''$ (J2000). The derived power spectral index for this field was $\beta = -2.82 \pm 0.01$ and the power at $k_0 = 0.1$ arcsec^{-1} is $P_0 = 0.223 \pm 0.007$ MJy sr^{-1}, much lower than in the galactic survey, where the lowest value measured was about $P_0 = 130$ MJy sr^{-1}. Using our formula, the confusion noise towards this field is $\sigma_{cn} = 0.09$ μJy, very close to the prediction.

4. Discussion

The main aims of the galactic FLS, viz the quick observing, processing, and release of characteristic views of our galaxy at mid- and far-infrared wavelengths, has been achieved. All the data was released to the public on April 22, 2004, four months after it was taken. The good agreement between the observed counts of point sources and SKY from 6^m to 15^m demonstrates that indeed typical regions around the galactic plane were selected which provide reliable information on source densities and confusion. Even at the large distances from the galactic center where the observations were made, confusion sets a limit to the detection of point sources in IRAC1 at 100 μJy $\approx 16.1^m$ (15.6^m for IRAC2) in the galactic plane. Only at latitudes larger than 10° did confusion noise not dominate the sensitivity of the IRAC1(2) images any more and we came close to the instrumental limit of 20 μJy $\approx 17.9^m$ (17.4^m for IRAC2).

Away from the galactic plane the effect of the warp of the galactic disk – a displacement to positive heights at longitudes near 90° – was clearly detected in the source counts. Shape and amplitude of the warp agree with an analysis of 2MASS data, after correcting for the fact that a larger galactocentric distance of the Sun (8.5 kpc) is assumed in the SKY model.

In the 24 μm GFLS, we measured a range in the spatial power spectral index from about $\beta = -2.2$ to -4.2. The average value was -2.9, similar to the normal index $\beta = -3.0$ used by Gautier et al. (1992) to estimate the 100 μm confusion noise. For some regions the index is constant from *IRAS*-accessible scales to the resolution of MIPS, implying that predictions based on lower resolution data are valid on small scales as well. In most regions, however, we detected a break such that the power spectrum becomes steeper for high wavenumber (small scales). This is fortuitous from the perspective of extragalactic observations since, for a given observational configuration, the confusion noise decreases when the cirrus power spectrum steepens.

Although the selection of the fields was not aimed at targets of particular interest, several new stellar clusters, HII-regions, and possibly a supernova remnant were easily detectable in the images. This demonstrates the great potential for discoveries with *Spitzer*.

Acknowledgements

We thank A. Noriega-Crespo for useful conversations.

References

Ábráham, P., Balázs, L.G., Kun, M. Morphology and kinematics of the Cepheus Bubble. A&A 354, 645–656, 2000.

Benjamin, R.A., Churchwell, E., Babler, B.L., et al. GLIMPSE. I. An SIRTF legacy project to map the inner galaxy. PASP 115, 953–964, 2003.

Burgdorf, M.J., Cohen, M., Price, S.D., et al. A survey of selected areas in the galactic plane with ISOCAM. A&A 360, 111–119, 2000.

Cohen, M. A model of the 2–35 micron point source infrared sky. AJ 105, 1860–1879, 1993.

Cohen, M. Powerful model for the point source sky: far-ultraviolet and enhanced midinfrared performance. AJ 107, 582–593, 1994.

Cohen, M. The displacement of the sun from the galactic plane using IRAS and FAUST source counts. ApJ 444, 874–878, 1995.

Diolaiti, E., Bendinelli, O., Bonaccini, D., et al. StarFinder: an IDL GUI-based code to analyze crowded fields with isoplanatic correcting PSF fitting. SPIE 4007, 879–888, 2000a.

Diolaiti, E., Bendinelli, O., Bonaccini, D., et al. Analysis of isoplanatic high resolution stellar fields by the StarFinder code. A&AS 147, 335–346, 2000b.

Dole, H., Lagache, G., Puget, J.-L. Predictions for cosmological infrared surveys from space with the multiband imaging photometer for SIRTF. ApJ 585, 617–629, 2003.

Drimmel, R., Spergel, D.N. Three-dimensional structure of the milky way disk: the distribution of stars and dust beyond $0.35\,R_{solar}$. ApJ 556, 181–202, 2001.

Fazio, G.G., Hora, J.L., Allen, L.E., et al. The infrared array camera (IRAC) for the spitzer space telescope. ApJS 154, 10–17, 2004.

Gautier, T.N., Boulanger, F., Pérault, M., et al. A calculation of confusion noise due to infrared cirrus. AJ 103, 1313–1324, 1992.

Ingalls, J.G., Miville-Deschênes, M.-A., Reach, W.T., et al. Structure and colors of diffuse emission in the spitzer galactic first look survey. ApJS 154, 281–285, 2004.

Kun, M., Balázs, L.G., Tóth, I. Giant infrared bubble in Cepheus. Ap&SS 134, 211–217, 1987.

López-Corredoira, M., Cabrera-Lavers, A., Garzón, F., et al. Old stellar Galactic disc in near-plane regions according to 2MASS: scales, cut-off, flare and warp. A&A 394, 883–899, 2002.

Lynds, B.T. Catalogue of dark Nebulae. ApJS 7 (1), 1962.

Marleau, F.R., Fadda, D., Storrie-Lombardi, L.J., et al. Extragalactic source counts at 24 microns in the spitzcr first look survey. ApJS 154, 66–69, 2004.

Padgett, D.L., Rebull, L.M., Noriega-Crespo, A., et al. An aggregate of young stellar disks in Lynds 1228 south. ApJS 154, 433–438, 2004.

Rebull, L.M., Stolovy, S., Karr, J., et al. Young Stellar Objects in the Spitzer galactic first look survey, in: Proceedings of the Second TPF Conference, http://planetquest1.jpl.nasa.gov/TPFDarwin-Conf/posterPapers.cfm, 2004.

Rho, J., Carey, S., Reach, W.T., et al. Infrared discovery of new HII regions and a possible supernova remnant in the spitzer galactic first look survey. BAAS 36, 724, 2004.

Rieke, G.H., Young, E.T., Engelbracht, C.W., et al. The multiband imaging photometer for spitzer (MIPS). ApJS 154, 25–29, 2004.

Schuller, F., Ganesh, S., Messineo, M., et al. Explanatory supplement of the ISOGAL-DENIS point source catalogue. A&A 403, 955–974, 2003.

Starck, J.-L., Murtagh, F. Automatic noise estimation from the multiresolution support. PASP 110, 193–199, 1998.

Wainscoat, R.J., Cohen, M., Volk, K., et al. A model of the 8–25 micron point source infrared sky. ApJS 83, 111–146, 1992.